ELSEVIER

Journal of Chromatography A, 695 (1995) 297–308

JOURNAL OF CHROMATOGRAPHY A

The separation of dihydrofolate reductase inhibitors and the determination of $pK_{a,1}$ values by capillary zone electrophoresis

Jing Cao, Reginald F. Cross*

School of Chemical Sciences Swinburne University of Technology John Street, Hawthorn, Vic. 3122, Australia

First received 23 September 1994; revised manuscript received 23 November 1994

Abstract

CZE was used as a method to separate eight dihydrofolate reductase inhibitors (DHFRI). Separation of the eight DHFRI was difficult to achieve and occurs only under very specific conditions. Baseline resolution occurred in 250 m*M* phosphate buffer of pH 2.1 at 13 kV. In an attempt to understand the mechanism of separation, $pK_{a,1}$ values have been determined and the effective hydrodynamic radii estimated by modeling the molecules. The consequential plot of Z/r versus the measured electrophoretic mobility gave a good linear correlation, thus demonstrating the fundamental nature of the separation mechanism.

1. Introduction

In the veterinary field, dihydrofolate reductase inhibitors (DHFRI) have acted as potentiators in combination with sulfonamides (SFA) for the prevention of bacterial and protozoal diseases of animals [1]. Although to a lesser degree, the same combinations are used in human medicine both in prophylactic and curative roles. There are three common DHFRI (trimethoprim, diaveridine and pyrimethamine) that have been used extensively and assays for these and the accompanying sulphonamide in urine, serum and animal tissues are scattered throughout the literature and continue to appear [2,3]. However, there are several other DHFRI that have either been used commercially with animals (ormetoprim) [1] or have been the subject of therapeutic studies in humans (brodimoprim) [4,5] and deposition and clearance studies in animals (ormetoprim) [6]. In addition, further DHFRI have been produced [1].

In total there appear [1] to have been eight DHFRI produced. They are pyrimethamine (PYR), diaveridine (DI), ormetoprim (OR), trimethoprim (TRI), aditoprim (ADI), metioprim (MET), tetroxoprim (TET) and brodimoprim (BRO).

If the eight are ever released for usage in the same market, the need for screening could arise. In this study we examine the suitability of capillary zone electrophoresis for that task. The general structures of the compounds is shown in Scheme 1 and the specific structural formula [1] and molecular masses are given in Table 1.

TRI has a pK_a of 6.6 and PYR has a pK_a of 7.0 [7]. The CZE behavior of these and DI in the vicinity of pH 8 clearly indicated [7] deprotona-

* Corresponding author.

0021-9673/95/$09.50
SSDI 0021-9673(94)01163-X

Table 1
Structural formulas and molecular masses for the eight dihydrofolate reductase inhibitors

DHFRI	n	R_1	R_2	R_3	R_4	M_r
Aditoprim	1	OCH_3	$N(CH_3)_2$	OCH_3	H	303.4
Pyrimethamine	0	H	Cl	H	CH_2CH_3	248.7
Diaveridine	1	OCH_3	OCH_3	H	H	260.3
Ormetoprim	1	CH_3	OCH_3	OCH_3	H	274.3
Brodimoprim	1	OCH_3	Br	OCH_3	H	339.2
Trimethoprim	1	OCH_3	OCH_3	OCH_3	H	290.3
Metioprim	1	OCH_3	SCH_3	OCH_3	H	306.4
Tetroxoprim	1	OCH_3	$OCH_2CH_2OCH_3$	OCH_3	H	334.4

tion to the electrically neutral form. It was observed that the easy separation of those three DHFRI may have been the fortuitous consequence of one of them being PYR. PYR is the only one of these three that is differently substituted in the pyrimidine ring where protonation can occur. Therefore it is the only DHFRI that could possibly carry a significantly different charge on the heterocycle. Of the other five, ADI is the only other drug that will be separable on the basis of total charge. The additional site for protonation on the basic dimethylamine substituent on the phenyl ring will ensure that ADI carries an additional charge at low enough pH. The other six will depend upon differences in size for variation in mobility and thus separation.

Consequently, it was not expected that CZE would easily separate these drugs. On the other hand, the plate counts achievable in CZE could enable the small size differences to be exploited.

2. Experimental

2.1. Instrumental

A Model 270 A CZE System by Applied Biosystems Inc. (Foster City, CA, USA) was used for all CZE experiments. The analytes were detected by UV–VIS absorbance at 225 nm. The detector time constant was set at 0.3 s in all experiments.

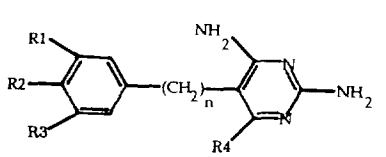

Scheme 1.

The determinations were performed on a 71.2 cm × 50 μm I.D. (220 μm O.D.) fused-silica capillary (Applied Biosystems) with the detection window located 52 cm from the injection end. The samples were injected at the anode (+) by vacuum injection for all analytes. All experiments were performed at 30° C. Electropherograms were recorded on a DeskJet Plus recorder and data were collected and integrated with a Model 270 capillary electrophoresis system interfaced to an Apple Macintosh computer. The 20 μm I.D. (350 μm O.D.) fused-silica capillary was supplied by J&W Scientific (Folsom, CA, USA). Its critical lengths were as for the 50 μm I.D. capillary.

2.2. Chemicals and materials

PYR, DI and TRI were obtained from Sigma (St. Louis, MO, USA), BRO was supplied by Helsinn (Biasca, Switzerland), and, ADI, MET, ORM and TET were provided by Hoffmann-La Roche (Basel, Switzerland). Standard stock solutions of each compound were prepared by precisely dissolving 0.1 g in 100 ml of HPLC grade methanol (BDH). Each compound was diluted with milli-q water to give a final concentration of 2.5 ng/μl. Sample solutions were filtered (0.45 μm) before injection. The neutral marker solution was prepared by weighing 0.1 g phenol and dissolving it in 1 l of HPLC grade methanol.

Phosphate buffers at 50–250 m*M* were prepared using Na_2HPO_4 and adjusted to the desired pH with 20% H_3PO_4 or 0.1 *M* NaOH. All chemicals were of AR grade and milli-q water was used to prepare all solutions.

2.3. Methods

Capillary preparation at the start of each day of experimentation involved initial purging with 0.1 *M* NaOH for 2 min, followed by milli-q water purging for 2 min and then with the running buffer for 2 min. Between the runs, the capillary was purged with 0.1 *M* NaOH for 2 min followed by running buffer for 2 min. Vacuum injections for 10 s were chosen to ensure signal-to-noise greater than 20:1. At the nominal 4 nl per second [8], 40 nl would have been injected. However, this nominal rate refers to water uptake. Hence the more viscous buffers used would lead to greatly reduced injection volumes. Furthermore, as the sample was dissolved in water, sample stacking compensates for this larger than usual volume.

3. Results and discussion

Given the apparent ease of separation of TRI, DI and PYR around pH 7 in 50 m*M* phosphate [7], these were the initial conditions chosen. However, in the vicinity of pH 6–7 with phosphate buffers, the doubly charged ADI is well resolved, but the remainder of the DHFRI comprised one broad band. Next we decreased the pH. The aim of these experiments was to decrease the electroosmotic flow and thereby permit differences in electrophoretic mobility to operate over an extended period. Fig. 1 shows the apparent mobilities. 50 m*M* phosphate buffer was used with 20 kV applied. It can be seen that the decrease in the apparent mobilities of the DHFRI follow that of the neutral marker but increased discrimination occurred. Fig. 2(a) shows the electropherogram at pH 2.1 where the resolution appeared to be marginally better than at surrounding pH values. With 20 kV applied, 50 m*M* NaCl–HCl solutions yielded similar resolution at pH 2, 3 and 4. At pH 1 no analyte peaks were observed. For $NaNO_3$–HNO_3 mobile phases, slightly inferior resolution was obtained and baseline noise was excessive.

At pH 2.1, with 50 m*M* phosphate buffers the effect of applied voltage was then examined. The results are shown in Fig. 3. There were not any significant changes in resolution over the voltage range examined. The only advantage observed was of reduced analysis times at higher applied voltages.

Fig. 4 shows the effect of phosphate buffer concentration on the apparent mobilities at pH 2.1 with 13 kV applied. With the higher buffer concentration, larger applied voltages led to the loss of all peaks. This was presumed to be due to Joule heating. As the maximum applied voltage for which peaks could be observed in 250 m*M* phosphate buffer was 13 kV, this voltage was chosen across the range of ionic strengths. It can be seen that the last pair of analytes (ORM, BRO) are finally separated in 250 m*M* phosphate buffer. Fig. 2 (b) shows the separation. In this high salt concentration (250 m*M*) the observed noise is many times larger than in the more normal range of buffer concentrations around 50 m*M* [see Fig. 2 (a)].

3.1. Buffer selection

In an attempt to effect separation at lower salt concentrations, we then tried some organic buffers. The commonly used buffers in the low pH range chosen were HCOOH–CH_3COOH pH 1.9 (24.4 ml, 90% and 87 ml, 99.8% respectively into 1 litre) and H_2NCH_2COOH–HCOOH pH 3.1 (0.1 *M* glycine, pH adjusted with HCOOH). The first of these is approximately 6 m*M* with respect to formate and 2 m*M* with respect to acetate whereas the glycine buffer is about 100 m*M*. At 13 kV, unfortunately only ADI was baseline resolved and the other seven DHFRI were combined in one broad, complex band in each case.

It may be that the brief search for a more dilute and less conducting buffer with appropriate selectivity was a futile exercise. It is notable in the work of Atamna et al. that it was

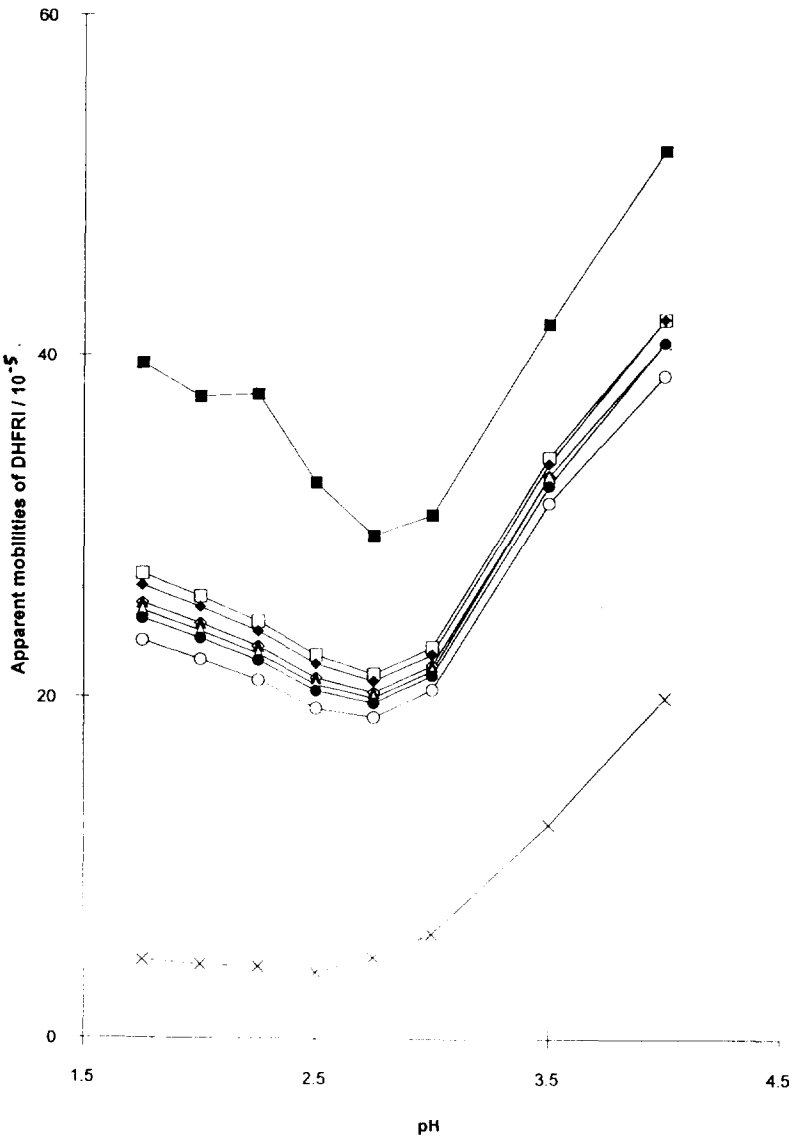

Fig. 1. Apparent mobilities ($cm^2 s^{-1} V^{-1}$) as a function of pH for the eight DHFRI (50 m*M* phosphate buffer at 20 kV). Legend: (■) ADI, (□) PYR, (◆) DIA, (◇) ORM, (▲) BRO, (△) TRI, (●) MET, (○) TET, (×) neutral marker.

the most highly conducting buffer that provided the best separations. When the role of the cation was examined, it was only in the most highly conducting cesium buffer where close to baseline resolution was observed. The lighter the alkali metal in the buffer, the further the separation deteriorated [9]. Similarly, when the role of the anion was isolated, the best resolution occurred in the most highly conducting citrate buffer, the worst resolution was observed in the least conducting bicarbonate buffer and the second least conducting acetate buffer had the second worst selectivity [10]. It has also been demonstrated that over a wide range of applied voltages resolution increases with increasing phosphate buffer concentration, up to 75 m*M* [11]. In the

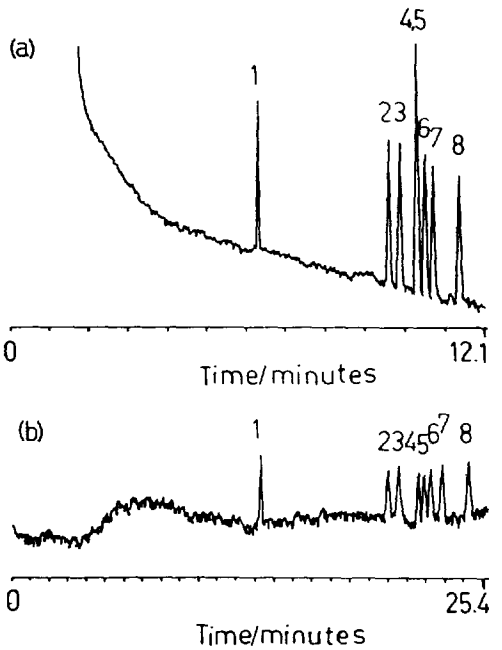

Fig. 2. Electropherograms of the eight DHFRI at pH 2.1. (a). In 50 m*M* phosphate buffer with 20 kV applied. (b). In 250 m*M* phosphate buffer with 13 kV applied.

current study, it is only in high concentration of the highly conducting phosphate buffer that all peaks are resolved. It therefore appears that at least for some classes of analytes there is a correlation between highly conducting buffers and increased selectivity. The consequence of this of course is that whilst a lowly conducting buffer such as lithium acetate may provide a good probe for Joule heating, it is likely to the worst choice for separation.

3.2. Peak loss

During the investigation there had been several sets of conditions under which all of the peaks had disappeared. Firstly, this occurred at 50 m*M* phosphate concentration with applied voltages greater than 25 kV. Secondly, for higher phosphate concentrations the peaks disappeared at progressively lower voltages. In the third instance, peaks were not observed for pH less than 1.75. In all of these cases the combination of high salt concentrations and/or high voltages indicated that excessive currents must have given rise to thermal mixing and dispersion. Unfortunately, currents were not automatically or systematically recorded. However, this seemed the most logical explanation. For the low pH solutions (1.75) the high concentration of protons in solution were probably the cause. This is consistent with observations by other workers restricting the practical pH range for CZE to 2–12 [12].

The other evidence for Joule heating lies in Fig. 3. Mobilities are known to increase by 2.7% per°C [13] due to the decreased viscosity and density of the supporting buffer [14]. For this reason, plots of mobility (both electroosmotic and electrophoretic) versus voltage are upward curving. The effects are more exaggerated at higher buffer concentrations and have been demonstrated very clearly [11]. Whilst the work of Issaq et al. [11] indicated the onset of this curvature above 50 m*M* buffer (for acetate at pH 5 and phosphate at pH 7), the effect is likely to be exacerbated for DHFRI in phosphate buffers at pH 2.1. As phosphoric acid has its $pK_{a,1}$ at 2.15 and the DHFRI have a $pK_{a,1}$ about 1 pH unit away (see next section) all mobilities will be heightened by increased dissociation as a result of Joule heating [11].

Thermal mixing

In view of the apparent heating problem leading to peak loss, it was decided to investigate the effect of decreasing the internal diameter of the capillary. Accordingly, the 20 μm I.D. capillary was obtained. It was hoped that better heat dissipation per cross-sectional area and would enable higher voltages to be applied, enabling quicker analyses to be achieved whilst maintaining baseline resolution of all analytes. Under the same conditions used for resolution of the sample previously (250 m*M* phosphate buffer, pH 2.1, 13 kV), no peaks were observed. This was totally unexpected and is contrary to the literature which indicates that Joule heating should not be a problem.

In the first instance, Knox [15] has calculated "Boundary conditions under which plate height contributions from thermal effects is less that 0.1

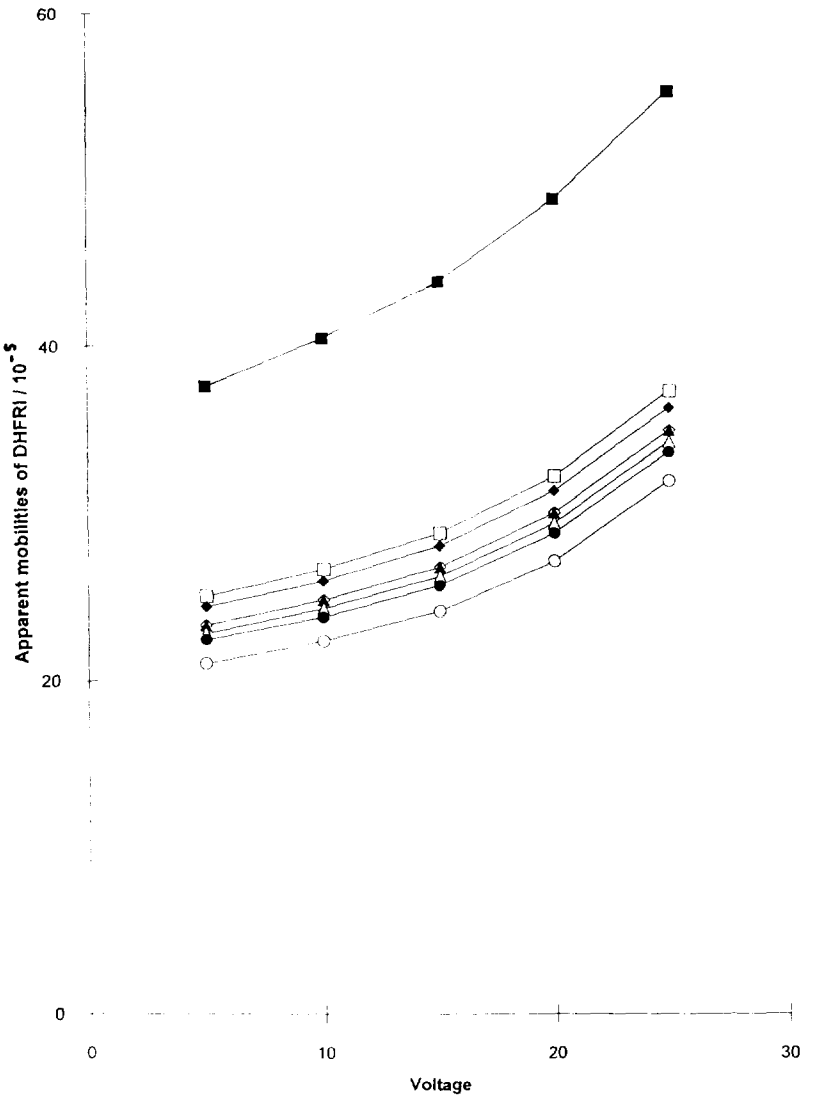

Fig. 3. Apparent mobilities ($cm^2\ s^{-1}\ V^{-1}$) as a function of voltage for the eight DHFRI (50 m*M* phosphate buffer at pH 2.1). Symbols as in Fig. 1.

times the plate height contribution from axial diffusion." A tabulation of limiting capillary diameters (d_c) for 10, 20, 50 and 100 kV m^{-1} across 10^{-3}, 10^{-2} and 10^{-1} mol dm^{-3} buffer solutions is given. Log–log plots of d_c versus buffer concentration are good linear plots for 10, 20 and 50 kV m^{-1} and were extrapolated to 0.25 mol dm^{-3}. The corresponding values of d_c, when plotted versus the applied voltage (V) on log–normal paper yielded a gently concave relationship. Interpolated to our applied voltage of 13 kV/0.712 m, the limiting diameter is 133 μm. Even allowing for the increased conductivity due to low pH, by a liberal extrapolation of the d_c versus V lines to 1 mol dm^{-2} buffer, the diameter for 10% increase in plate height is still 83 μm. (Our capillary was 50 μm diameter).

Similarly, Gruska et al. [16] have estimated that for small molecules in 0.1 *M* buffers there will be negligible loss in HETP for capillaries

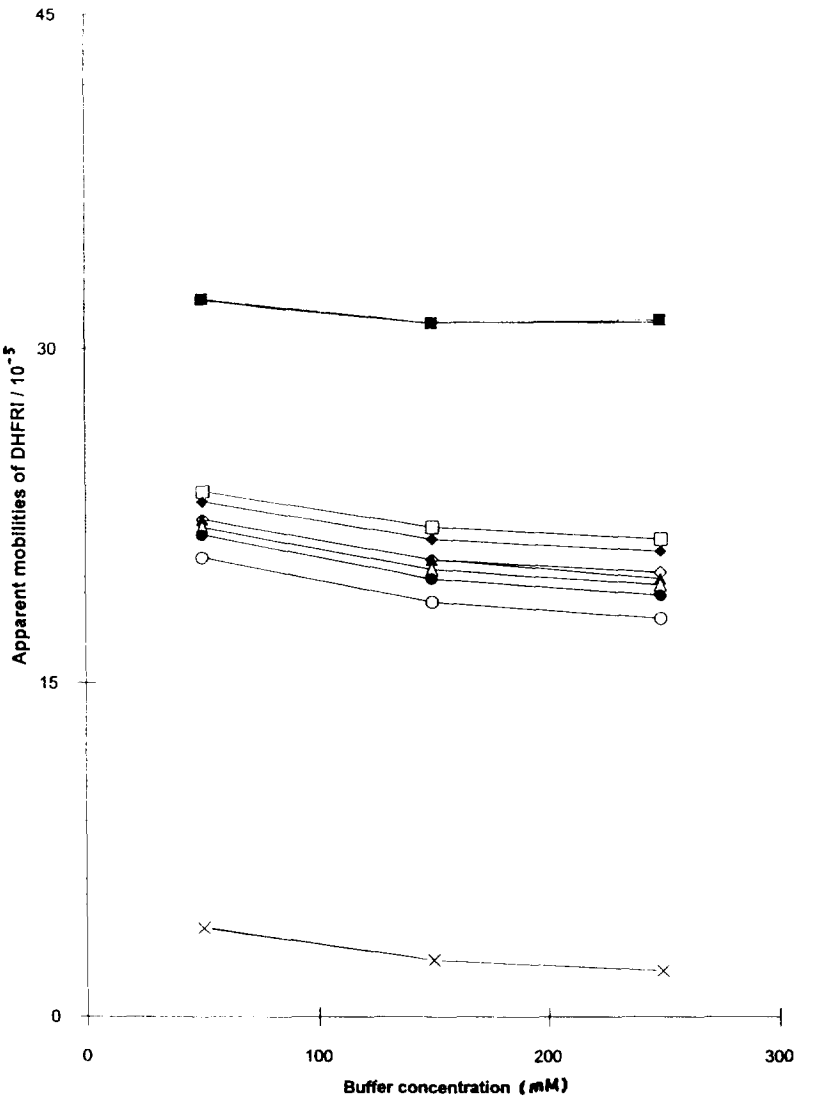

Fig. 4. Apparent mobilities ($cm^2 s^{-1} V^{-1}$) as a function of concentration of buffer for the eight DHFRI (with 13 kV at pH 2.1). Symbols as in Fig. 1.

between 50 and 100 μm internal diameter with 30 kV m^{-1} applied and analyte velocities in the range of 1–10 cm min^{-1}. Plate losses are greatest at the highest velocities, but are still negligible. For 50 μm I.D. capillaries at approximately 4 cm min^{-1} (typical for our analyses), the HETP is clearly coincidental with the theoretical curve of maximum efficiency.

Thus the available evidence in the literature appears to deny significant loss of efficiency due to Joule heating under our experimental conditions. The only possible additional factor that requires some examination is the effect of the greater overall diameter and wall thickness in the case of the 20 μm I.D. capillary. (See Instrumental section.) The 20 μm I.D. capillary has a semi-insulating coating of 165 μm of fused silica compared to 85 μm around the 50 μm I.D. capillary. However, with the thermal conductivity of the capillary wall being far greater than that

of buffer solutions [16], conventional wisdom is that this will not cause excessive Joule heating to occur [17].

Adsorption

The alternate explanation for peak losses is adsorption. Loss of proteins on the walls of fused-silica capillaries has been recognized as a problem in CZE from very early on [19]. The technique proposed to avoid this was to coat the wall and thereby prevent interaction with the ionized negatively charged silanols. Alternate approaches involve adjustment of the pH to values above the p*I* for the proteins to ensure net negative charge and repulsion from the capillary walls or to use swamping concentrations of strong electrolytes to saturate adsorption sites in the electrical double layer [20].

In the case of small (non zwitterionic) molecules, another alternative is to adjust the pH to yield electrically neutral species and use micellar electrokinetic capillary chromatography (MECC). However, CZE is simpler and will therefore be preferred if adsorption is avoided.

The acid–base properties of silica have been well understood for a long time [21]. The pK_a for the silanols is between 6 and 7 and the potential of zero charge is at about pH 2. Consequently, electrostatic adsorption of cationic species on the silica walls would be expected to increase in proportion to surface charge with increasing pH, if permissible under the given conditions. In fact a water soluble, non surfactant, polymeric cation (trimethylammonium glycol chitosan iodide) has been shown to adsorb on silica in a fashion that exactly mirrors the increase in charge density on silica gel between pH 3.5 and 10 [22]. In this case, negligible adsorption was indicated in the lower pH range. On the other hand, in 10 m*M* NaBr C_{14}TAB exhibits decreasing adsorption from pH 6 down but appears to flatten out well above zero in the vicinity of pH 2 [23]. Also, in the case of polyvinylimidazole (a cationic polyelectrolyte with p$K_a \sim 5$), similar behavior versus pH is observed up to the region of the pK_a, but at low pH the extent of adsorption is strongly dependent upon ionic strength [24]. Contrary to expectations [25], the extent of adsorption increases with NaCl concentration. More importantly, the trend in the data with pH allows for finite adsorption in the vicinity of pH 2. As imidazoles are 1,3-dinitrogen heteroaromatics, this data is particularly relevant. With similar chemistry and charge distribution, similar behavior may be expected of the DHFRI.

There are several other factors to be considered in conjunction with the possibility of the adsorption of the DHFRI on silica at low pH. Firstly, at the potential of zero charge (pH $\sim$ 2), it is the net charge that is zero. There will be negative (and positive) charges on the surface. Secondly, the extent of ionization of the surface silanols is increased by adsorption. In solution-depletion experiments involving large surface areas of silica and small volumes of C_{14}TAB in 10 m*M* NaBr, the bulk solution is observed to proportionately decrease in pH [23]. Clearly, the process must be viewed as ion exchange rather than simple adsorption. Thirdly, with a pK_a in the vicinity of 1, the DHFRI will be more strongly preferred counter ions for exchange as the pH approaches 1. Fourthly, it is known that maximal adsorption of carboxylic acids and amines occurs for pHs around the pK_a [21]. This is presumed to be due to the favorable energetics of the proton exchange mechanism. This leads to the last salient point which is that non electrostatic adsorption due to strong hydrogen bonding on the surface is also possible. Increasing adsorption due to this mechanism might be expected as the pH approaches the potential of zero charge for the silica (around 2).

For the 20 μm I.D. capillary, the increased internal surface area-to-volume ratio in the smaller I.D. capillary, the smaller radial distances of diffusion to the walls and the reduced sample size (at fixed injection interval) would all facilitate adsorption.

In the absence of more definitive evidence the above indicates that DHFRI adsorption is a distinct possibility from electrolyte solutions at low pH. However, the significance of these equilibrium studies to flowing solutions in CZE will also depend upon adsorption kinetics.

The simplest way to test for adsorption would be to substitute a coated capillary in place of the

untreated silica under otherwise identical conditions. The appearance of peaks would then strongly indicate adsorption, whilst their continued absence would tend to deny it.

3.3. Migration order

To understand the order of migration of the eight analytes we have looked to the basics of the migration process. The electrophoretic mobility, μ_{ep} is given [14] by Eq. 1:

$$\mu_{ep} = Z/(6\pi\eta r) \quad (1)$$

where Z is the effective charge on the ion, η is the viscosity and r is the hydrodynamic radius. For any prescribed condition of separation, η will be fixed and therefore the order of separation will depend only upon Z and r. We therefore set out to determine these values for the analytes.

Determination of Z

As the successful separation of the eight analytes occurred at pH 2.1, it is there that the calculations have been done.

For all of the DHFRI we can write the ionic equilibria as shown in Scheme 2.

Analysis of the hydrogen bonding and molecular packing of DHFRI and related compounds by Cody et al. [26], and by others, using computational methods and crystal structure determinations leave little doubt that the preferred site for protonation is on the N1 (ring nitrogen). These give rise to the $pK_{a,2}$ values between 6 and 7 and full protonation at pH 2.1. As with many nitrogen heterocycles, $pK_{a,1}$ values are expected around 1 or 2 [27] and in the case of the DHFRI it is expected that protonation will occur at the N3 position [26]. Overall then we expect that the DHFRI will have a net charge of 1.x in general around pH 2.1.

For ADI there is also the additional protonation on the dimethylammonium group on the phenyl ring (see Scheme 3).

We do not have a value for this pK_a, but reference to the available data allows an estimate to be made [28]. Aniline has a pK_b of 9.38 whereas o-methoxy aniline has a pK_b of 9.51. Hence we assume that the pK_b of aniline derivatives will have their pK_b values increased by 2×0.13 due to disubstitution by methoxy groups in the ortho positions. Similarly, N,N-dimethyl substitution of aniline leads for an increase in pK_b of $+0.22$. Given that the pK_b for *p*-methylaniline is 9.00, the pK_b for 2,6-dimethoxy-4-methyl-(N,N-dimethylaniline) will be approximately $9.00 + 0.22 + 0.26 \sim 9.48$ and $pK_{a,3}$ (ADI) ~ 4.52. While this estimate is clearly qualitative, it does indicate that the remaining pK_a for ADI is probably significantly above 2.1 and that we may assume full protonation at pH 2.1.

To determine the fraction of protonation due to the $pK_{a,1}$ we have used the method of Beckers et al. [18]. The two solutions used to determine $pK_{a,1}$ were 250 m*M* phosphate buffer at pH 2.1 with 13 kV applied and 50 m*M* phosphate buffer at pH 3.5 with 15 kV applied. Due to the lower limitation on the useful range of pH for CZE, it was not feasible to go to lower pH [12]. Table 2 shows the raw data from which the calculation were done.

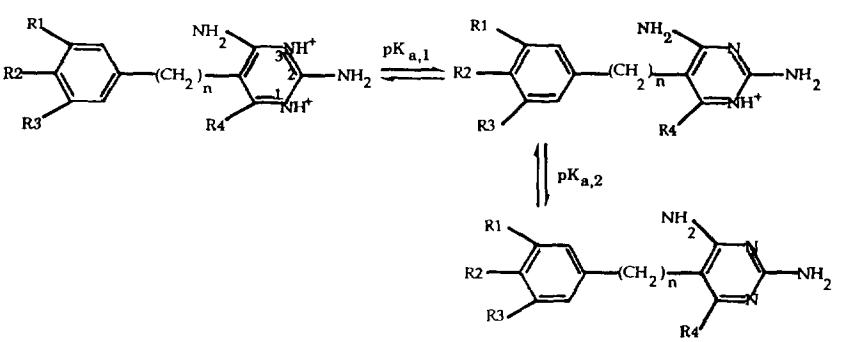

Scheme 2.

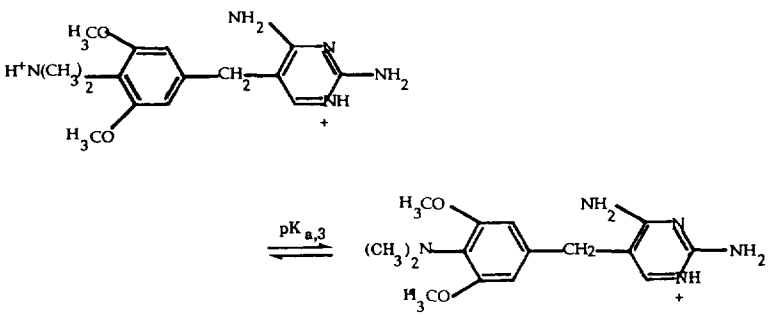

Scheme 3.

Table 2
Apparent migration times for the DHFRI and the neutral marker (minutes) and calculated pK_a values

DHFRI	Migration time		pK_a
	pH 2.1	pH 3.5	
Aditoprim	15.755	10.31	1.065
Pyrimethamine	22.44	14.38	1.2334
Diaveridine	22.99	14.645	1.2441
Ormetoprim	24.065	15.125	1.2758
Brodimoprim	24.375	15.125	1.3401
Trimethoprim	24.7	15.325	1.3234
Metioprim	25.295	15.59	1.3361
Tetroxoprim	26.64	16.245	1.3418
Neutral marker	169.52	49.205	–

The Debye–Hückel expression for activity coefficients was used as in Beckers et al. [18]. The effective hydrodynamic radii used were those calculated in the next section and shown in Table 3. The calculated pK_a values are given in the final column of Table 2.

Determination of r

Prior to determining values of r, the molecular masses of the DHFRI were used as a first approximation to the relative molecular volumes. This proportionality has previously led to a good correlation between electrophoretic mobility and "charge to mass" ratio [7]. However, in that case the analytes under consideration were sulphonamides and the majority of heteroatom variations from carbon were nitrogens and oxygens with approximately the same atomic density. For the DHFRI, BRO is clearly an outlier in any such calculation due to the exceptionally high density of the bromine atom.

Initial attempts to determine r were based upon physical model building with spheres. However, imprecision in size scaling of the

Table 3
Values used in the calculation of Z/r and its correlation with μ_{ep}

DHFRI	Z	r	Z/r	μ_{ep}
Aditoprim · $2H_2O$	2.083	3.107	0.67	27.33
Pyrimethamine · H_2O	1.12	2.738	0.409	18.35
Diaveridine · H_2O	1.122	2.85	0.394	17.85
Ormetoprim · H_2O	1.13	2.856	0.396	16.92
Brodimoprim · H_2O	1.148	2.962	0.388	16.67
Trimethoprim · H_2O	1.143	2.921	0.391	16.42
Metioprim · H_2O	1.147	2.96	0.388	15.97
Tetroxoprim · H_2O	1.149	3.153	0.364	15.02

atoms and the bond lengths led us to look for a more precise method of estimation.

The Sybyl 6.01 molecular modeling software was used to obtain minimum energy configurations of the eight DHFRI with a water of hydration added to each of the fully protonated sites; that is, one water of hydration at the N1 site for all DHFRI and a second water of hydration on the dimethylammonium site for ADI.

As there was no mechanism in the software for calculating an averaged radius, we initially used the cross-sectional area of the molecule when the charge (or charges in the case of ADI) were to the forefront dragging the molecule through the solution. These areas were estimated from printouts of the appropriately averaged electron cloud diagram with a superimposed angstrom grid. Values so determined led to correlations which appear to deny the validity of an electrostatically enforced preferred ionic orientation in the electric field during migration.

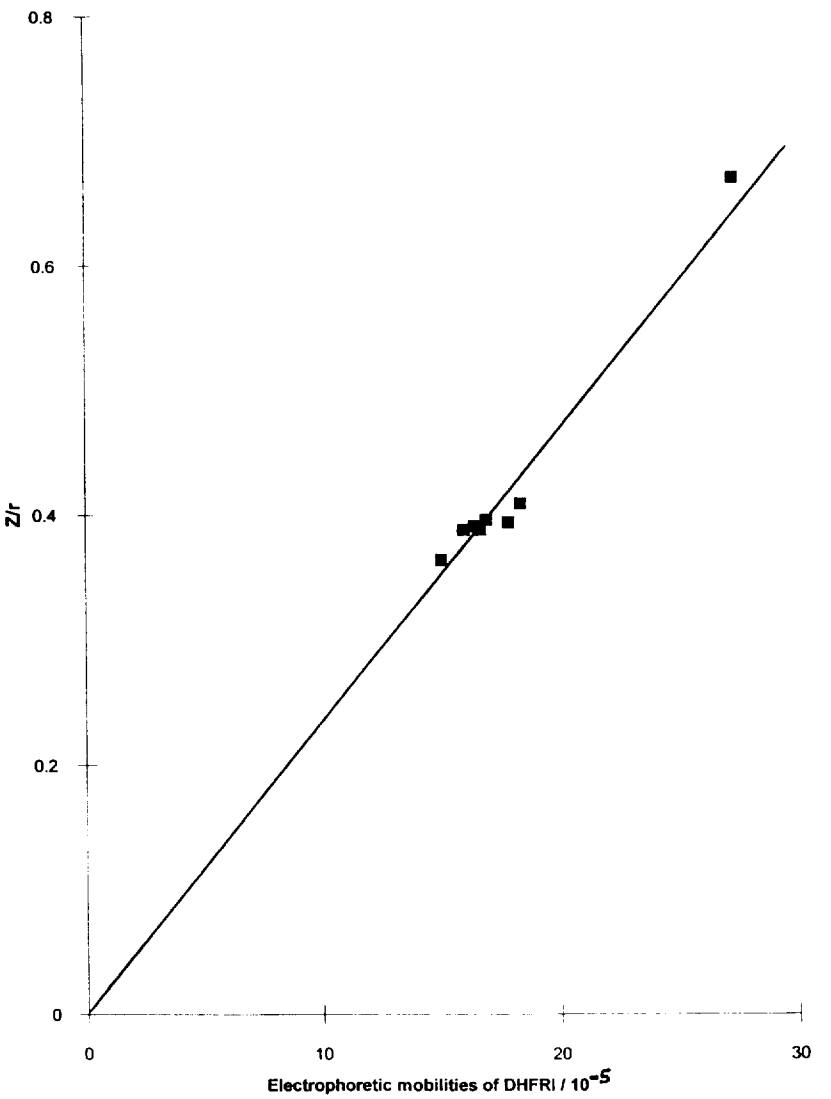

Fig. 5. Z/r values as a function of electrophoretic mobilities ($cm^2\ s^{-1}\ V^{-1}$). Symbols as in Fig. 1.

Since there was not any measurement of volume available we opted for the "contact" surface area from which the radius of an equivalent sphere was calculated. The data are given in Table 3.

Correlation

Table 3 shows the data used to calculate Z/r and the values of electrophoretic mobilities of the ions. Fig. 5 shows the plot of Z/r versus electrophoretic mobilities. From a least squares regression the correlation coefficient is 0.980. In general, the compliance of the data with Eq. 1 is quite good and the order of migration appears to be determined primarily by the fundamental molecular properties of charge and size.

The spread of the data about the line of best fit is likely to arise from both possible sources of errors; the values of pK_a and of r. In the case of pK_a, the inability to do experiments at a sufficiently low pH will contribute to less precise values of pK_a. Also, estimates of the activity coefficients in the method of pK_a calculation will be approximate due to the use of the Debye–Hückel expression up to ionic strengths of 0.25. For r, the modeling package is likely to yield an extremely accurate approximation to the molecule, but our usage of the contact surface to calculate the radii of equivalent spheres may not be as a good an approximation to the effective hydrodynamic radius in all cases.

Acknowledgements

We thank Hoffmann-La Roche for the donation of four of the DHFRI, and Helsinn for the donation of brodimoprim. We also thank Ashley Mansell for his experimental support, Dr. Margaret Wong for her help with the molecular modeling and Dr. Ian Harding of the centre for Applied Colloid Science, Swinburne for useful discussions regarding adsorption.

References

[1] W.F. Rehm, K. Teelmann and E. Weidekamm, in A.G. Rico (Editor), *Drug Residues in Animals*, Academic, Orlando, FL, 1986, Ch. 4.

[2] M.M. Lemnge, A. Ronn, H. Flachs and I.C. Bygbjerg, *J. Chromatogr.*, 613 (1993) 340–346.

[3] P. Nachilobe, J.O. Boison, R.M. Cassidy and A.C.E. Fesser, *J. Chromatogr.*, 616 (1993) 243–252.

[4] H.J. Laurencot, A. Schlosser and J.L. Hempstead, *Poult. Sci.*, 51 (1972) 1181–1187.

[5] E. Weidekamm, E. Eschenhof, B. Weber and A. Darragh, in K.H. Spitzy and K. Karrer (Editors), *Proceedings of the 13th International Congress on Chemotherapy, Vienna*, 1983, Egerman, Vienna, p. 59/1.

[6] E. Werner, A. Braunsteiner, F. Finsinger and Z. Maric, in K.H. Spitzy and K. Karrer (Editors), *Proceedings of the 13th International Congress on Chemotherapy, Vienna*, 1983, Egerman, Vienna, p. 59/16.

[7] M.C. Ricci and R.F. Cross, *J. Microcol Sep.*, 5 (1993) 207–215.

[8] *Model 270A User's Manual*, Applied Biosystems, Santa Clara, CA, 1989.

[9] I.A. Atamna, C.J. Metral, G.M. Muschik and H.J. Issaq, *J. Liq. Chromatogr.*, 13 (1990) 2517–2527.

[10] I.A. Atamna, C.J. Metral, G.M. Muschik and H.J. Issaq, *J. Liq. Chromatogr.*, 13 (1990) 3201–3210.

[11] H.J. Issaq, I.Z. Atamna, G.M. Muschik and G.M. Janini, *Chromatographia*, 32 (1991) 155–161.

[12] J.A. Cleveland, Jr., M.H. Benko, S.J. Gluck and Y.M. Walbroehl, *J. Chromatogr A.*, 652 (1993) 301–308.

[13] S. Hjerten, *Electrophoresis*, 11 (1990), 665–690.

[14] R.J. Wieme, in E. Heftmann (Editor), *Chromatography: A Laboratory Handbook of Chromatographic and Electrophoretic Methods*, Van Nostand Reinhold, New York, 3rd ed., 1975, p. 267.

[15] J.H. Knox, *Chromatographia*, 26 (1968) 329–337.

[16] E. Gruska, R.M. McCormick and J.J. Kirkland, *Anal. Chem.*, 61 (1989) 241–246.

[17] M. Verhoef, personal communication.

[18] J.L. Beckers, F.M. Everaerts and M.T. Ackermans, *J. Chromatogr.*, 537 (1991) 407–428.

[19] J.W. Jorgenson and K.D. Lukacs, *Science*, 222 (1983) 266–272.

[20] S.F.Y. Li, *Capillary Electrophoresis*, Elsevier, Amsterdam, 1992.

[21] T.W. Healy, *J. Macromol. Sci. - Chem.*, A8 (1974) 603–619.

[22] E. Kokufuta, S. Fujii, Y. Hirai and I. Nakamura, *Polymer*, 23 (1982) 452–456.

[23] P. Wangnerud and G. Olofsson, *J. Colloid Interface Sci.*, 153 (1992) 392–398.

[24] B. Popping, A. Deratani, B. Sebille, N. Desbois, J.M. Lamarche and A. Foissy, *Colloids Surfaces*, 64 (1992) 125–135.

[25] I.H. Harding, personal communication.

[26] C.H. Schwalbe and V. Cody, in J.A. Blair (Editor), Proceedings of the *7th International Symposium on Structural Studies of Antifolate Drugs, Birmingham, 1982*, de Gruyter, Berlin, 1983, pp. 511–515.

[27] D.D. Perrin, *Dissociation Constants of Organic Bases in Aqueous Solution*, IUPAC, Butterworths, London, 1965 and 1972.

[28] P. Sykes, *A Guidebook to Mechanism in Organic Chemistry*, Longmans, London, 1961.